Journal of Biological Engineering

https://doi.org/10.1186/s13036-026-00711-3

Article in Press

Unravelling the metabolism of itaconate and related branched C5-dicarboxylates for CO_2-based production in *Cupriavidus necator* H16

Received: 1 April 2026

Accepted: 6 June 2026

Published online: 13 June 2026

Cite this article as: Hanko E.K.R. & Malys N. Unravelling the metabolism of itaconate and related branched C5-dicarboxylates for CO_2-based production in *Cupriavidus necator* H16. *J Biol Eng* (2026). https://doi.org/10.1186/s13036-026-00711-3

Erik K. R. Hanko & Naglis Malys

Unravelling the metabolism of itaconate and related branched C5-dicarboxylates for CO_2-based production in *Cupriavidus necator* H16

Erik K. R. Hanko[a,b], Naglis Malys[c,d]*

[a]BBSRC/EPSRC Synthetic Biology Research Centre (SBRC), School of Life Sciences, The University of Nottingham, Nottingham, NG7 2RD, United Kingdom

[b]Manchester Institute of Biotechnology, Faculty of Science and Engineering, University of Manchester, 131 Princess Street, Manchester, M1 7DN, United Kingdom

[c]Bioprocess Research Centre, Faculty of Chemical Technology, Kaunas University of Technology, Radvilenu st. 19, LT-50254 Kaunas, Lithuania

[d]Department of Organic Chemistry, Faculty of Chemical Technology, Kaunas University of Technology, Radvilenu st. 19, LT-50254 Kaunas, Lithuania

*Author to whom correspondence should be addressed: n.malys@gmail.com

Abstract

Branched C5-dicarboxylates (C5-DCAs), such as itaconate, are high-value platform chemicals with diverse applications in the synthesis of bio-based polymers. In addition to their industrial relevance, itaconate has attracted attention as a key immunomodulatory metabolite. In this study, we demonstrated that *Cupriavidus necator* can grow on itaconate as its sole carbon source and identified key genes involved in its degradation through targeted deletions. These include multiple functional homologs of itaconate CoA-transferase, itaconyl-CoA hydratase, and (*S*)-citramalyl-CoA lyase, which

collectively mediate itaconate catabolism. We also identified ItcR1, a LysR-type transcriptional regulator, as a key mediator of itaconate-responsive gene expression. Transcriptomic analysis revealed broader transcriptional responses to itaconate, methylsuccinate, and mesaconate, suggesting an expanded role of C5-DCA metabolism. Finally, by expressing a heterologous *cis*-aconitate decarboxylase, we achieved the autotrophic production of a C5-DCA mixture of methylsuccinate, citramalate, mesaconate, and itaconate from CO_2 and hydrogen. These findings provide new insight into branched C5-DCA metabolism in *C. necator* and advance its development as a chassis for the sustainable production of these industrially relevant compounds from inorganic feedstocks.

Keywords: *Cupriavidus necator*, carbon dioxide, bioproduction, biomanufacturing, itaconate, methylsuccinate, C5-DCA

Introduction

Branched C5-dicarboxylates (C5-DCAs), and particularly itaconate, have emerged as molecules of interest due to their anti-inflammatory and antimicrobial roles[1, 2]. Moreover, as a non-toxic and sustainable substitute for petroleum-derived monomers, itaconate has been recognised by the U.S. Department of Energy as a top value-added chemical derived from biomass[3], providing an alternative to acrylate and methacrylate. Owing to its two carboxyl groups and a double bond, itaconate can easily be transformed into a wide array of compounds via simple reduction, amination, and decarboxylation reactions, and it can be used as a versatile building block

for the synthesis of polymers employed in paints, adhesives, latex, gel coats, superabsorbent polymer materials, plastics, and resins[4-7]. Since there is no chemical synthesis route established, itaconate is currently produced at industrial scale through microbial fermentation of carbohydrates, primarily using fungi such as *Aspergillus terreus*[8, 9], reaching titres exceeding 100 g/L[10]. In the last decade, efforts have also focused on expanding production to alternative microbial hosts and organic carbon sources[11-16].

While organic carbon and energy sources such as glucose and xylose are widely used as substrates in biomanufacturing processes due to their accessibility, they are typically derived from food crops or lignocellulosic biomass. This not only introduces competition for arable land but also necessitates agricultural product- or waste-processing[17]. In contrast, carbon dioxide (CO_2) is an abundant and readily available inorganic carbon source, and hydrogen (H_2) is considered a clean energy carrier that can be produced from renewable sources. Together, these inorganic feedstocks present a promising alternative that supports carbon neutrality and energy security, reduces environmental impact, and decouples production from agricultural inputs. This approach is especially well-suited for the microbial biosynthesis of platform chemicals such as itaconate, potentially offering a more sustainable route to their industrial production.

Autotrophic microorganisms such as *Cupriavidus necator* H16 are particularly promising in this context, as they can fix CO_2 using H_2 as an energy source. Beyond CO_2 fixation, *C. necator* is an attractive microbial

chassis for industrial applications due to its genetic tractability, metabolic versatility, and capacity to redirect metabolic flux from native poly-3-hydroxybutyrate (PHB) biosynthesis toward value-added platform chemicals[18]. For example, engineered strains of *C. necator* have achieved the autotrophic production of compounds such as 1,3-butanediol, 2,3-butanediol, isopropanol, D-mannitol, and mevalonate[19-22].

While itaconate can be biosynthesised from the tricarboxylic acid cycle intermediate *cis*-aconitate or its isomer *trans*-aconitate through a single enzymatic reaction[8, 13], it can also be broken down and reintegrated into primary metabolism. The canonical itaconate degradation pathway consists of three enzymatic steps: first, itaconate is activated to its CoA ester by itaconate CoA-transferase (Ict); next, itaconyl-C4-CoA is hydrated to (3*S*)-citramalyl-CoA by itaconyl-CoA hydratase (Ich); and lastly, (3*S*)-citramalyl-CoA is cleaved into pyruvate and acetyl-CoA by (*S*)-citramalyl-CoA lyase (Ccl, Figure 1)[23, 24]. The genes encoding Ict, Ich, and Ccl enzymes were first identified in *Yersinia pestis* and *Pseudomonas aeruginosa*[25], where they are organised into operons that are transcriptionally induced in response to itaconate[26]. While the *Y. pestis* operon encodes only the core Ict, Ich, and Ccl enzymes, the *P. aeruginosa* operon encodes three additional proteins, two of which, a methylsuccinyl-CoA dehydrogenase (Mcd) and a (*S*)-(*R*)-methylsuccinate or -methylsuccinyl-CoA isomerase (MmgE/PrpD), enable (*R*)- and (*S*)-methylsuccinate to feed into the same catabolic route (Figure 1)[25, 27, 28]. In addition, in *Burkholderia xenovorans*, a mesaconate hydratase has

been shown to catalyse the hydration of mesaconate to (*S*)-citramalate, thereby providing the enzymatic step required for mesaconate to enter this degradation pathway in this bacterium[29]. Similar to other metabolically versatile soil bacteria such as *Pseudomonas fluorescens* and *B. xenovorans*, *C. necator* harbours a gene cluster resembling the six-gene itaconate degradation operon of *P. aeruginosa*, albeit with only five homologous genes[25]. Three enzymes encoded within this cluster – MmgE/PrpD, Ict, and Mcd – have recently been shown to collectively facilitate the conversion of both (*S*)- and (*R*)-methylsuccinate into mesaconyl-C4-CoA in *C. necator*[30]. However, despite these insights, the broader metabolism of itaconate and related branched C5-DCAs, and the genetic basis underlying this process, remain poorly understood in *C. necator*.

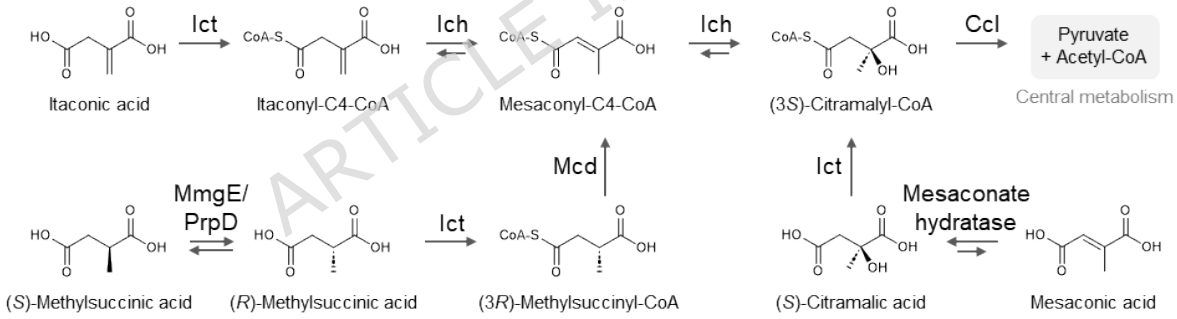

Figure 1. Routes of branched C5-DCA metabolism. Enzyme abbreviations: Ict, itaconate CoA-transferase; Ich, itaconyl-CoA hydratase; Ccl, (*S*)-citramalyl-CoA lyase; Mcd, methylsuccinyl-CoA dehydrogenase; MmgE/PrpD family protein, (*S*)-(*R*)-methylsuccinate isomerase.

In this study, we explore the capacity of *C. necator* to degrade itaconate and identify the genetic and regulatory elements underlying this process. We demonstrate that *C. necator* can utilise itaconate as its sole carbon source

and that this ability is linked to multiple gene clusters encoding homologs of known itaconate-degrading enzymes. Through systematic gene deletions and promoter-reporter assays, we show that operons encoding Ict, Ich, and Ccl homologs play cumulative roles in itaconate catabolism, while additional, previously uncharacterised genes contribute to the interconversion of branched C5-DCAs. Furthermore, we identify ItcR1, a LysR-type transcriptional regulator, as a key mediator of gene expression in response to itaconate. Transcriptomic analysis reveals a broader set of genes inducible by itaconate, methylsuccinate, and mesaconate, expanding the known landscape of branched C5-DCA metabolism in bacteria. Leveraging these insights, we engineer a *C. necator* strain to produce a mixture of branched C5-DCAs from CO_2 by expressing a heterologous *cis*-aconitate decarboxylase from *Aspergillus terreus*. This work lays the foundation for future metabolic engineering of *C. necator* for the CO_2-based biosynthesis of itaconate and related C5-DCAs.

Methods

Microbial strains

E. coli TOP10 (Life Technologies) was employed for cloning and plasmid propagation, while *E. coli* S17-1 λpir served as conjugation donor[31]. *C. necator* H16 and its derivatives were used to investigate C5-DCA metabolism and biosynthesis. All bacterial strains were routinely propagated in lysogeny broth (LB)[32]. Low-salt LB (LSLB)-MOPS was employed for conjugative plasmid transfer, gene deletion, and gene replacement[33]. The investigation

of itaconate metabolism and biosynthesis, promoter-reporter assays, and transcriptome analysis in *C. necator* were conducted in chemically defined minimal medium (MM)[34] supplemented with 1 mL/L trace element solution SL7[35], and optionally sodium gluconate or itaconate as the carbon source. When appropriate, antibiotics were added to the medium at the following concentrations: tetracycline (12.5 µg/mL for *E. coli* or 15 µg/mL for *C. necator*), chloramphenicol (25 µg/mL for *E. coli* or 50 µg/mL for *C. necator*), or gentamycin (10 µg/mL). For solid media preparation, 15 g/L agar was added. *E. coli* was routinely grown at 37℃, while *C. necator* was cultured at 30℃.

Cloning and transformation

Plasmid DNA was extracted using the QIAprep Spin Miniprep Kit (Qiagen). *C. necator* genomic DNA was isolated using the GenElute Bacterial Genomic DNA Kit (Sigma-Aldrich). Oligonucleotide primers were synthesised by Sigma-Aldrich and are listed in Table S1. DNA for cloning was amplified by PCR in 50-µL reactions using Phusion High-Fidelity polymerase (New England Biolabs, NEB). Colony PCR, employed for screening successful gene deletions or replacements, was performed in 25-µL reactions using the DreamTaq Green PCR Master Mix (2X, Thermo Fisher). Gel-purified linearised DNA was extracted using the Zymoclean Gel DNA Recovery Kit (Zymo Research). Restriction enzymes, T4 DNA ligase, and the NEBuilder HiFi DNA Assembly Master Mix were purchased from NEB. All PCR, digestion, and ligation reactions were set up according to the manufacturer's

protocol. Chemically competent *E. coli* were prepared and transformed by heat shock[32]. Plasmids based on pBBR1MCS were transformed by electroporation following the method reported by Ausubel et al.[36], while pLO3-derived vectors were transformed into *C. necator* by conjugation[33].

Plasmid and strain construction

Plasmids were constructed using either conventional restriction enzyme-based cloning[32] or HiFi DNA Assembly. Intergenic regions used for promoter-reporter gene fusions were amplified from *C. necator* genomic DNA and cloned into pEH006 digested with AatII and NdeI[37]. Plasmids used for gene deletions or genomic integration of *cadA* were based on the suicide plasmid pLO3[33].

For gene deletions, vector constructs included homology arms of roughly 1000 bp, corresponding to the regions upstream and downstream of the target gene, designed to delete the entire coding sequence. For genomic integration of the itaconate biosynthesis pathway, a plasmid carrying the *A. terreus cadA* gene under the control of a heterologous L-arabinose inducible system was used. This construct was flanked by homology arms matching the upstream and downstream region of the *phaCAB* locus.

All plasmids were verified by Sanger sequencing (Source BioScience, Nottingham). Detailed plasmid assembly descriptions are provided in the Supplementary Methods, and an overview of the plasmids used and generated in this study is summarised in Table S2. Gene deletions and integrations were performed following a method reported previously[33].

Briefly, plasmids for gene deletions and integrations were transferred from *E. coli* S17-1 into *C. necator* H16 by conjugation. Transconjugants were selected on fructose-MM (0.4%) agar supplemented with 15 µg/mL tetracycline and 10 µg/mL gentamycin, purified twice by restreaking on fructose-MM agar, and incubated overnight in LSLB-MOPS without antibiotics. Approximately 10^8 cells were then plated onto LSLB agar containing 15% sucrose to select for sucrose-resistant survivors that had lost the pLO3 plasmid. Successful strain construction was confirmed by colony PCR using the oligonucleotide primers listed in Table S3.

Itaconate consumption assay

To quantify itaconate consumption by wild-type *C. necator* H16, single colonies from freshly streaked plates were used to inoculate 5 mL of MM containing 0.4% (w/v) sodium gluconate (SG-MM) and gentamycin. Cultures were grown in 50-mL conical centrifuge tubes at 30℃ with shaking at 200 rpm. From the overnight culture, cells equivalent to 0.6 OD_{600} units were harvested by centrifugation at 10,000 *g* for 5 min. Subsequently, the cell pellet was resuspended in 6 mL of MM containing either 11 mM gluconate or 9 mM itaconate.

To monitor itaconate metabolism in deletion strains, single colonies were inoculated into 5 mL of LB with gentamycin and incubated overnight under the same conditions. The next day, 5 mL of SG-MM were inoculated 1:100 with the overnight culture and incubated for 24 hours. Main cultures were then prepared by diluting the seed cultures 1:50 into 6 mL of fresh SG-

MM. After 4 hours of incubation, itaconate was added to a final concentration of 5 mM. Cell growth was monitored by measuring absorbance at 600 nm, and concentrations of gluconate and C5-DCAs were determined by high-performance liquid chromatography (HPLC).

Metabolite quantification

For HPLC analysis, cell-free culture supernatants were mixed with an equal volume of mobile phase, which was spiked with 50 mM valerate as an internal standard. The aqueous mobile phase consisted of 5 mM H_2SO_4. The mixture was then filtered through a 0.22 µm cellulose acetate syringe filter. HPLC analysis was performed using a Thermo Scientific UltiMate 3000 HPLC system equipped with a Phenomenex Rezex ROA-organic acid H+ (8%) column (150 mm × 7.8 mm, 8 µm), a DAD-3000 diode array detector set to 210 and 280 nm, and a RefractoMax 521 refractive index detector (Thermo Fisher Scientific). The mobile phase was delivered isocratically at a flow rate of 0.5 mL/min, with the column maintained at 35℃. A 20 µL injection volume was used and samples were run for 30 min. Peak areas were integrated using Chromeleon 7 software (Thermo Fisher Scientific), and metabolite concentrations were quantified based on calibration curves generated from standards of known concentration. Representative HPLC chromatograms of standards are shown in Figure S1.

Fluorescence measurements

For promoter-reporter assays, single colonies of freshly transformed wild-type *C. necator* or strain EHCn13 were inoculated into 2 mL of SG-MM

supplemented with chloramphenicol and grown overnight in 50-mL conical centrifuge tubes at 30℃ with shaking at 200 rpm. Main cultures were prepared by diluting the overnight seed cultures 1:20 into 5 mL of fresh SG-MM with chloramphenicol and incubated under the same conditions. At an OD_{600} of 0.2, 142.5 µL of exponentially growing cells was transferred to a 96-well microtitre plate (flat, clear bottom, black; Greiner Bio-One). To each well, 7.5 µL of stock inducer was added to reach a final concentration of 5 mM. The plate was then placed in a Tecan Infinite M1000 PRO microplate reader and incubated at 30℃ with orbital shaking at 408 rpm. Red fluorescent protein (RFP) fluorescence was measured using excitation and emission wavelengths of 585 and 620 nm, respectively. Culture absorbance at 600 nm was used to normalise fluorescence by cell density. Prior to normalisation, both fluorescence and absorbance readings were background-corrected by subtracting values from cell-free medium. Normalised fluorescence was determined six hours after inducer addition.

Autotrophic production of C5-DCA

For the autotrophic production of C5-DCAs in strain EHCn14, single colonies from freshly streaked plates were used to inoculate 3 mL of SG-MM supplemented with gentamycin. Cultures were grown in 50-mL conical centrifuge tubes at 30℃ with shaking at 200 rpm for 36 hours to ensure complete consumption of sodium gluconate, therefore preventing carryover of organic carbon into the autotrophic production medium. From the resulting seed culture, cells equivalent to 0.8 OD_{600} units were harvested by

centrifugation at 10,000 *g* for 5 min. The cell pellet was then resuspended in 10 mL of MM and transferred to 250-mL serum bottles. The headspace was filled with a gas mixture of H_2, CO_2, and air in a ratio of 8:1:1 (v/v/v)[38], and the cultures were incubated under the same conditions. To induce *cadA* expression, 0.5 mL of MM containing L-arabinose (final concentration of 0.5 mM) was injected into each bottle 22 hours after culture initiation, ensuring that cells were in the logarithmic growth phase at the time of induction. At the same time, an additional 50 mL of air was added to the headspace. Samples of 0.5–1 mL were collected at defined time points to monitor cell growth and quantify C5-DCA titres. It should be noted that L-arabinose was not consumed by *C. necator* H16 as a carbon or energy source.

Transcriptome analysis

To investigate the transcriptional response of wild-type *C. necator* to itaconate, methylsuccinate, and mesaconate, two individual colonies grown on solid SG-MM were each used to inoculate 5 mL of SG-MM with gentamycin in 50-mL conical centrifuge tubes. Cultures were incubated overnight at 30℃ with orbital shaking at 200 rpm. The following day, main cultures were prepared by diluting the seed cultures 1:50 into 6 mL of fresh SG-MM containing gentamycin. After six hours of incubation under the same conditions, cultures were supplemented with itaconate, methylsuccinate, or mesaconate to a final concentration of 5 mM. An untreated culture (gluconate only) served as a control. Following an additional six hours of incubation – by which time cultures had reached an OD_{600} of 0.4–0.6 – cells equivalent to one

OD_{600} unit were harvested and immediately stabilised using RNAprotect Bacteria Reagent (Qiagen), according to the manufacturer's instructions. It should be noted that only insignificant growth rate variations were observed depending on supplement added to the culture. The resulting cell pellets were flash-frozen in liquid nitrogen and stored at −80°C until RNA extraction.

Total RNA was isolated using the Qiagen RNeasy Mini Kit, and residual DNA was removed using the TURBO DNA-free Kit (Thermo Fisher), following the respective manufacturer protocols. RNA integrity and concentration were determined using an Agilent 2100 Bioanalyzer. Prokaryotic RNA library preparation, sequencing, and bioinformatic analysis were performed by Novogene (Cambridge, UK).

Differential expression analysis was performed using a significance threshold of $p < 0.05$ ($n = 2$ biological replicates). Genes meeting this criterion were considered differentially expressed relative to the untreated control.

Sequence databases and BLAST analysis

Nucleotide and protein sequences were retrieved from the National Center for Biotechnology Information (NCBI) database. BLASTp[39], available on the NCBI website, was used to identify protein homologs.

Quantification and statistical analysis

Statistical analyses were performed using two-tailed *t*-tests, with statistical significance defined as $p < 0.05$. The number of biological replicates (n) is

provided in each figure legend. Data in all graphs are presented as mean ± standard deviation.

Results

C. necator H16 can utilise itaconate as the sole carbon source

To enable itaconate production in *C. necator*, it was first essential to determine whether the compound is catabolised and how this pathway might impact target product formation. In a previous study, we identified a gene cluster in *C. necator* exhibiting significant similarity with the itaconate degradation pathway found in *P. aeruginosa* PAO1[26]. This cluster encodes homologs of the itaconate coenzyme A (CoA) transferase (Ict), itaconyl-CoA hydratase (Ich) and (*S*)-citramalyl-CoA lyase (Ccl), hereafter referred to as Ict1, Ich1, and Ccl1, respectively (Figure 2A). Furthermore, it encodes two additional enzymes that are also found in the itaconate degradation gene cluster of *P. aeruginosa*. The first enzyme exhibits high homology with the product of PA0879, a methylsuccinyl-CoA dehydrogenase (Mcd) that catalyses the conversion of (3*R*)-methylsuccinyl-CoA into mesaconyl-C4-CoA[27, 28]. The second enzyme shares high homology with the product of PA0881, a member of the MmgE/PrpD protein family, which functions as an (*S*)-(*R*)-methylsuccinate isomerase, enabling both enantiomers of methylsuccinate to enter the degradation pathway.

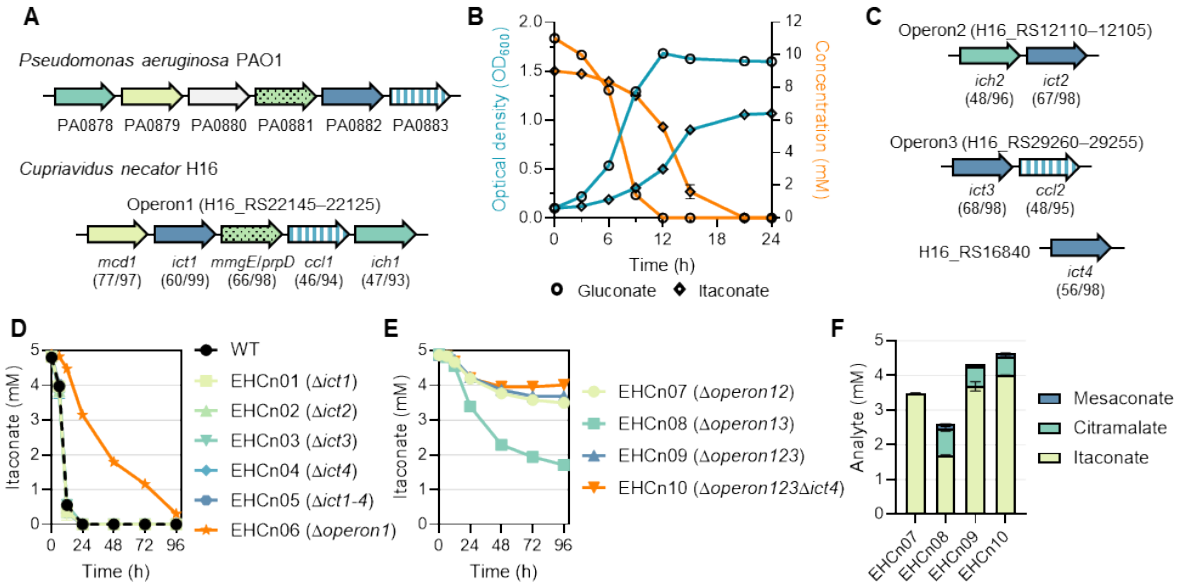

Figure 2. Itaconate utilisation in *C. necator* H16. a Illustration of gene clusters encoding the complete itaconate degradation pathways in *P. aeruginosa* PAO1 and *C. necator* H16. Locus tags, gene names, and protein sequence homologies (% identity / % coverage) are indicated. Genes are not drawn to scale. **b** Growth of wild-type *C. necator* H16 in minimal medium (MM) supplemented with either gluconate (circles) or itaconate (diamonds) as the sole carbon source. Culture absorbance (blue curves) and carbon source concentration (orange curves) were monitored over 24 hours. **c** Gene cluster organisation of Operon2, Operon3, and gene H16_RS16840, encoding homologs of *P. aeruginosa* PA0882 (Ict) with over 40% protein sequence identity. Locus tags, gene names, and protein sequence homologies (% identity / % coverage) are indicated. Genes are not drawn to scale. **d** Itaconate consumption by wild-type *C. necator* (WT) and its derivative strains EHCn01–06. Cells were grown in gluconate-MM supplemented with 5 mM itaconate. **e** Itaconate consumption by strains EHCn07–10 under the same growth conditions as in panel **d**. **f** Composition of C5-DCAs in the culture supernatants of strains EHCn07–10 grown in gluconate-MM, 96 hours after supplementation with 5 mM itaconate. Data represent the mean ± standard deviation (n = 3). Error bars may be too small to be visible in some cases.

Given that *C. necator* possesses all the necessary genes for itaconate catabolism, we examined whether this bacterium can utilise itaconate as the sole carbon source. To test this, cells grown in gluconate-minimal medium (MM) were resuspended in MM supplemented with itaconate (itaconate-MM), and the growth of wild-type *C. necator* was monitored over a 24-h period. While growth in itaconate-MM was notably slower compared to cells grown in gluconate-MM (Figure 2B), indicating an adjustment period when switching between carbon sources, itaconate was completely consumed, and the cell culture reached maximum cell density within 21 hours. This confirms the capability of *C. necator* to utilise itaconate as the sole carbon source.

Deletion of *ict1–4* does not affect itaconate degradation

A BLASTp search revealed the existence of four homologs of *P. aeruginosa* PAO1 Ict in the genome of *C. necator*, exhibiting protein sequence identities greater than 40% and coverages of 98% or higher. Additionally, the genome encodes an extra five Ict homologs with protein sequence identities ranging from 35% to 40% and coverages of 96% or higher (Table S4). Alongside these identified Ict homologs, *C. necator* possesses two homologs each of *P. aeruginosa* Ich and Ccl. Except for gene *H16_RS16840*, referred to as *ict4*, the second Ich and Ccl homologs are encoded in separate operons, each clustered with one of the highly similar Ict homologs (Figure 2C). Given that the deletion of *ict* in *P. aeruginosa* isolate 605 led to the loss of its ability to use itaconate as a sole carbon source[40], we conducted individual and combined deletions of the genes encoding Ict1–4 in order to determine their

involvement in itaconate catabolism in *C. necator*. Surprisingly, the individual deletion of *ict1–4*, as well as their combined deletion (yielding strain EHCn05, Table 1), exhibited no significant impact on itaconate degradation (Figure 2D). In all strains, itaconate was completely consumed within 24 hours. This observation raises the possibility that itaconate might be activated by CoA-transferases with lower homology to *P. aeruginosa* Ict, the degradation of itaconate might proceed through alternative pathways involving either a CoA-ligase or a lyase-type enzyme acting on itaconate, or potentially a combination of both.

The gene clusters encoding Ict1–3 play a cumulative role in itaconate metabolism

Given that the deletion of *ict1–4* did not exhibit any influence on curtailing itaconate catabolism, we turned our attention to deleting *H16_RS22120–H16_RS22145*, hereafter referred to as *operon1*, which encodes Ict1, Ich1, Ccl1, Mcd1, and the (*S*)-(*R*)-methylsuccinate isomerase (Figure 1 and 2A). Notably, deletion of *operon1* (designated as strain EHCn06) significantly affected itaconate consumption. In contrast to the wild-type strain, which consumed 5 mM of itaconate entirely within 24 hours, strain EHCn06 retained over 60% of itaconate unconsumed after the same time period (Figure 2D). While the consumption rate of itaconate was considerably reduced, confirming the involvement of *operon1* in itaconate metabolism, this observation suggested that Ich1 and Ccl1 are not the sole enzymes with itaconyl-CoA hydratase and (*S*)-citramalyl-CoA lyase activities, respectively.

To investigate the role of the gene clusters encoding Ich2 and Ccl2, we performed individual and combined deletions of *operon2* and *operon3* in strain EHCn06. The deletion of *operon2*, encoding Ict2 and Ich2 (yielding strain EHCn07, Table 1), further reduced *C. necator*'s ability to consume itaconate. In contrast to strain EHCn06, where nearly all itaconate was consumed within 96 hours, almost 70% of itaconate remained unconsumed in the supernatant of strain EHCn07 cultures (Figure 2E). A similar reduction in itaconate consumption was observed in strain EHCn08 (Δ*operon1* and Δ*operon3*), although to a lesser extent than in strain EHCn07 (Figure 2E). However, the deletion of Ict3 and Ccl2 led to the accumulation of 0.14 mM mesaconate and 0.76 mM citramalate in the culture medium (Figure 2F), both being products of itaconate degradation that had not accumulated in strains EHCn01–07. This indicates that even in the absence of both Ich homologs in strain EHCn07, itaconate is still degraded into intermediates of central metabolism (Figure 1), with Ccl2 playing a role. Nonetheless, deletion of both operons harbouring *ccl* genes, either partially or entirely, abolishes itaconate consumption via (3*S*)-citramalyl-CoA, resulting in the accumulation of citramalate and mesaconate (Figure 1). It should be noted that mesaconate and citramalate are released from mesaconyl-CoA and (3*S*)-citramalyl-CoA, respectively, to regenerate CoA, as observed previously[25].

Table 1. Strains used and generated in this study.

Strain	Parental strain	Genotype/description	Reference or source

E. coli			
TOP10	-	F⁻ *mcrA* Δ(*mrr-hsdRMS-mcrBC*) φ80*lacZ*ΔM15 Δ*lacX74 recA1 araD139* Δ(*ara-leu*)*7697 galU galK* λ⁻ *rpsL*(Str^R) *endA1 nupG*	Life Technologies
S17-1 λpir	-	*thi pro hsdR*⁻ *hsdM*⁺ recA *RP4-2(Tc::Mu, Km::Tn7)* λpir TpR SmR	[31]
C. necator			
H16	-	Wild type strain (DSM 428)	DSMZ
EHCn01	H16	Δ*ict1*	This study
EHCn02	H16	Δ*ict2*	This study
EHCn03	H16	Δ*ict3*	This study
EHCn04	H16	Δ*ict4*	This study
EHCn05	EHCn01	Δ*ict2* Δ*ict3* Δ*ict4*	This study
EHCn06	H16	Δ*operon1* (Δ*ict1* Δ*ich1* Δ*ccl1* Δ*mcd1* Δ*mmgE/prpD*)	This study
EHCn07	EHCn06	Δ*operon2* (Δ*ict2* Δ*ich2*)	This study
EHCn08	EHCn06	Δ*operon3* (Δ*ict3* Δ*ccl2*)	This study
EHCn09	EHCn07	Δ*operon3* (Δ*ict3* Δ*ccl2*)	This study
EHCn10	EHCn09	Δ*ict4*	This study
EHCn11	EHCn10	Δ*mcd2*	This study
EHCn12	EHCn10	Δ*sucCD*	This study
EHCn13	H16	Δ*itcR1*	This study
EHCn14	EHCn11	Δ*phaCAB* P_{araC}-*araC* P_{araBAD}-*cadA*	This study

To evaluate the cumulative effect of *operon1–3* on itaconate metabolism, we generated a triple knockout strain (yielding strain EHCn09, Table 1). Both effects observed in strains EHCn07 and EHCn08 were also apparent in strain EHCn09; itaconate consumption was considerably reduced, accompanied by the accumulation of 0.09 mM mesaconate and 0.56 mM citramalate in the

culture medium (Figure 2E and 2F). Even less itaconate was consumed in strain EHCn10, in which *operon1–3* were deleted, along with the last remaining Ict homolog (Figure 2E). In this strain, 95% of the initially added itaconate remained in the culture medium as a mixture of 4.0 mM itaconate, 0.54 mM citramalate, and 0.1 mM mesaconate (Figure 2F). Furthermore, as itaconate activation by succinyl-CoA synthetase has been reported in *Advenella mimigardefordensis* strain DPN7^{T}[41], we tested whether this reaction could contribute to residual itaconate conversion in *C. necator*. To this end, we deleted *sucCD* in strain EHCn10, yielding strain EHCn12. However, deletion of *sucCD* had no detectable effect on itaconate consumption or on citramalate and mesaconate accumulation, with extracellular metabolite titres indistinguishable from those observed in strain EHCn10. On this basis, strain EHCn12 was not analysed further. The persistence of the conversion of itaconate into mesaconate and citramalate in strain EHCn10, despite the deletion of all predicted Ict, Ich, and Ccl homologs, indicates the presence of promiscuous enzymatic activities in *C. necator* that facilitate the interconversion of branched C5-DCAs. For example, a potential contribution of enzymes involved in TCA cycle and C4-DCA metabolism, which exhibit hydratase and dehydrogenase activities, cannot be ruled out.

Deletion of *mcd1* and *mcd2* results in the accumulation of methylsuccinate

To gain deeper insights into the interplay between the various gene clusters during itaconate metabolism, we constructed promoter-reporter gene fusions

and quantified the reporter output in response to itaconate, citramalate, mesaconate, and methylsuccinate. Methylsuccinate was included as inducer because *operon1* encodes all the necessary enzymes for the conversion of methylsuccinate into pyruvate and acetyl-CoA (Figure 1 and 2A). In addition to the promoters of *operon1–3* and *ict4*, we also included the promoter of gene *H16_RS25540*. This particular gene encodes the protein with the highest homology to the Mcd from *P. aeruginosa* PAO1, exhibiting a protein sequence identity of 79% and a coverage of 99% (referred to as Mcd2 hereafter). Among the tested promoter-reporter gene fusions, $P_{operon1}$ demonstrated the most substantial induction in response to itaconate (Figure 3A), displaying an 81-fold induction of reporter output. Moreover, the same promoter exhibited a 62-fold induction in the presence of methylsuccinate and a 3-fold induction with mesaconate, while citramalate failed to mediate reporter gene expression.

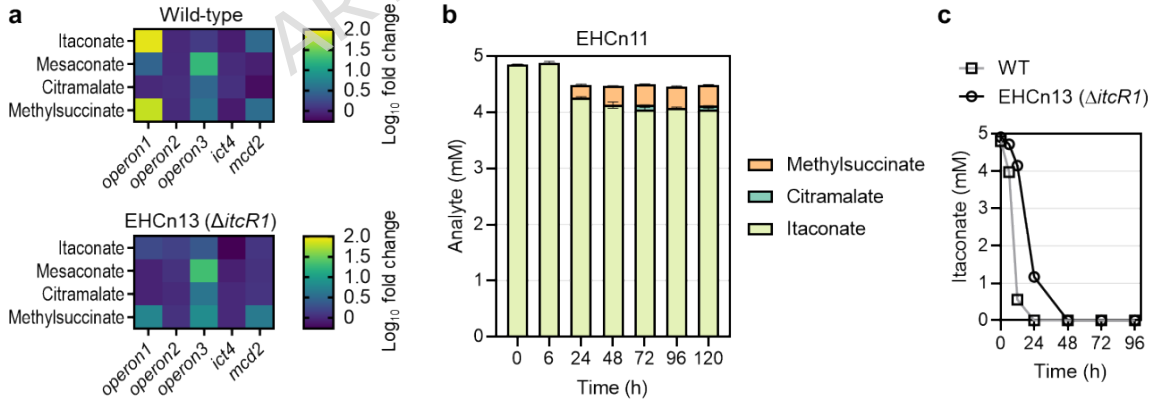

Figure 3. Roles of ItcR1 and Mcd2 in itaconate metabolism. a Promoter activity in wild-type *C. necator* and strain EHCn13 (Δ*itcR1*) in response to itaconate, mesaconate, citramalate, and methylsuccinate. Reporter output from promoter-reporter fusions was quantified six hours after addition of

each C5-DCA at a final concentration of 5 mM. **b** Composition of C5-DCAs in the culture supernatant of strain EHCn11 grown in gluconate-MM. Itaconate was added at time zero to a final concentration of 5 mM. **c** Itaconate consumption by strain EHCn13 grown in gluconate-MM supplemented with 5 mM itaconate. Data represent the mean ± standard deviation ($n = 3$). Error bars may be too small to be visible in some cases.

The strong activation of the promoter of *operon1* by both itaconate and methylsuccinate underscores its role in the metabolism of these two compounds. Likewise, the activation of the promoter of gene *H16_RS25540* (*mcd2*) by itaconate and methylsuccinate, each resulting in a 3-fold induction, provides further evidence of the involvement of both Mcd1 and Mcd2 in channelling methylsuccinate into the same degradation pathway as itaconate. In fact, the deletion of *mcd2* in strain EHCn10 (resulting in strain EHCn11) led to the accumulation of methylsuccinate in the culture medium, while the levels of citramalate and mesaconate decreased considerably compared to strain EHCn10 (Figure 3B). This observation implies the roles of Mcd1 and Mcd2 in catalysing the conversion of (3*R*)-methylsuccinyl-CoA into mesaconyl-C4-CoA. Intriguingly, this finding also suggests that a certain proportion of the branched C5-DCA pool is converted into methylsuccinate.

In contrast to the promoters of *operon1* and *mcd2*, which were predominantly activated by itaconate and methylsuccinate, the promoter of *operon3* – encoding Ict3 and Ccl2 – exhibited the highest induction level in response to mesaconate (17-fold). It was also activated by methylsuccinate, citramalate, and itaconate, though to a lesser extent (4-, 3-, and 1.3-fold, respectively; Figure 3A). Its strong activation by mesaconate, along with considerably

lower induction by the other compounds tested, suggests that *C. necator* may have acquired Ict3 and Ccl2 as an independent catabolic unit, enabling it to specifically metabolise mesaconate and citramalate.

The promoters of *operon2* and *ict4* demonstrated no significant induction in response to any of the four tested compounds, instead mediating a constitutive level of gene expression, with P_{ict4} exhibiting the lowest level of reporter gene expression (Table S5).

ItcR1 is involved in mediating gene expression in response to itaconate

In a previous study, we established that the promoter controlling the expression of itaconate degradation pathway genes in *P. aeruginosa* PAO1, referred to as P_{ich}, is induced in response to itaconate[26]. This activation of gene expression was shown to be mediated by the transcriptional regulator PaItcR, which is encoded in the opposite orientation to the *P. aeruginosa* itaconate degradation gene cluster. Surprisingly, even in the absence of PaItcR, we observed that expression from P_{ich} remained induced upon exposure to itaconate in wild-type *C. necator*, but not in *Escherichia coli*[26]. This intriguing observation implied the involvement of a transcriptional regulator endogenous to *C. necator* in facilitating gene expression from the heterologous promoter[26]. Although a similar genetic arrangement featuring a transcriptional regulator protein encoded in the opposite orientation of *operon1* was not evident in *C. necator*, we identified a LysR-type transcriptional regulator situated nearby on the same strand as *operon1*.

The regulator protein encoded by gene *H16_RS22160* exhibits homology with PaItcR, demonstrating a protein sequence identity of 42% and a coverage of 97%. Given its close proximity to *operon1* and its considerable homology to PaItcR, we deleted gene *H16_RS22160* in wild-type *C. necator*, resulting in strain EHCn13. In this new strain, the induction of expression from the promoters of *operon1* and *mcd2* in response to itaconate was almost entirely abolished (Figure 3A). Noticeably, while the response of the *operon1* promoter to methylsuccinate was reduced by 11-fold, the *mcd2* promoter remained largely unaffected, exhibiting only a slight 1.3-fold increase. These findings indicate that the transcriptional regulator encoded by gene *H16_RS22160* (hereafter referred to as *itcR1*) primarily governs the regulation of *operon1* and *mcd2* expression in response to itaconate. However, it appears that the expression of these genes in response to methylsuccinate is either partially (in case of *operon1*) or fully (in case of *mcd2*) controlled by another unknown transcriptional regulator. Furthermore, the deletion of *itcR1* did not affect the induction of expression of *operon3*, suggesting that another unknown transcriptional regulator is implicated in the mesaconate-responsive activation of gene expression. Although the deletion of *itcR1* notably influenced the consumption of itaconate (Figure 3C), its efficacy in slowing down itaconate degradation was less pronounced compared to strain EHCn06 (Figure 2D). This indicates that even the minimal expression of *operon1* in the absence of the itaconate-bound ItcR1 is adequate to facilitate itaconate consumption.

Identification of additional genes putatively involved in branched C5-DCA metabolism

Up to this point, a strain unable to completely consume itaconate was constructed; nevertheless, itaconate was still undergoing conversion into other C5-DCAs, namely methylsuccinate, citramalate, and mesaconate. To gain a more comprehensive understanding of the additional genes encoding enzymes potentially involved in the interconversion of these branched C5-DCAs within *C. necator*, we performed a transcriptomic analysis on the wild-type strain, which was cultivated in the presence of itaconate, methylsuccinate, or mesaconate. This analysis enabled us to identify an array of distinct genes and gene clusters whose expression was upregulated due to the presence of these compounds. All genes showing at least a fourfold increase in expression in response to at least one of the three inducers ($p < 0.05$) are illustrated in Figure 4 (Table S6). The outcome of the transcriptomic analysis validates the findings from the promoter-reporter gene induction assays. For example, the genes within *operon1* and *mcd2* were among the most significantly induced genes in response to itaconate and methylsuccinate, but not mesaconate. Similarly, the expression of *operon3*, encoding Ict3 and Ccl2, was predominantly induced by mesaconate and, to a lesser degree, by methylsuccinate, while remaining unaffected by itaconate.

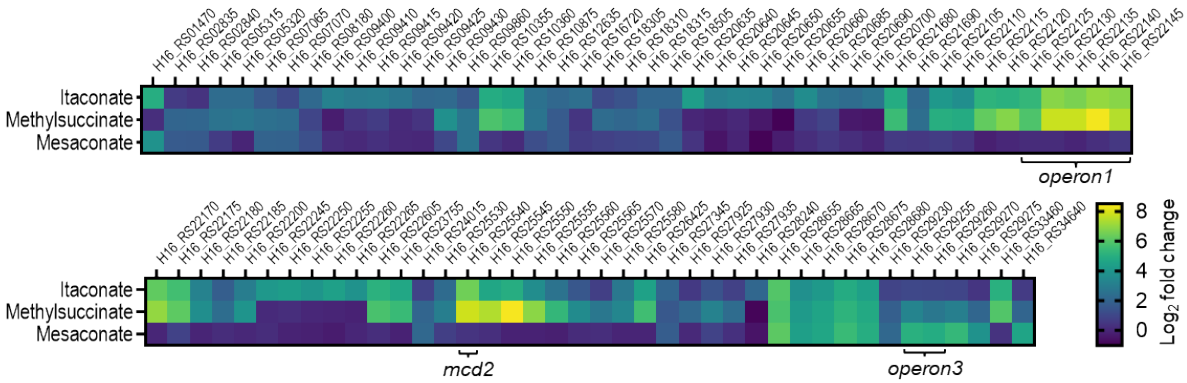

Figure 4. Transcriptomic changes of wild-type *C. necator* in response to itaconate, methylsuccinate, and mesaconate. Genes shown are those differentially expressed relative to the untreated control ($p < 0.05$; $n = 2$) and exhibiting at least a fourfold increase in expression in response to at least one of the three inducers. Genes are ordered by ascending locus tag.

Interestingly, the presence of mesaconate only led to the induction of a limited subset of genes, which stands in contrast to itaconate and methylsuccinate, both of which triggered the upregulation of a considerable number of genes and gene clusters. This finding implies the existence of an extensive network of enzymes that may potentially be implicated in the metabolism of itaconate and methylsuccinate. For instance, gene clusters *H16_RS20635–20660* and *H16_RS22245–22265* exhibited enhanced expression due to itaconate, while remaining unaffected by the other two compounds. Both of these gene clusters encode enzymes with predicted functions akin to those encoded by *operon1*, encompassing CoA transferases and acyl-CoA transferases. In addition, gene clusters *H16_RS10355–10360* and *H16_RS22115–22120*, both of which include genes encoding putative CoA-ligases, exhibited elevated expression in response to itaconate and methylsuccinate. Although these enzymes might not process itaconate as

efficiently as the enzymes encoded by *operon1*, they could still contribute to itaconate metabolism to some extent. Moreover, the transcriptomic analysis unveiled the upregulated expression of a diverse array of genes associated with transport functions, offering potential targets for future metabolic engineering endeavours focused on exploring branched C5-DCA transport.

Engineering *C. necator* for the autotrophic production of itaconate

Because of itaconate's potential as a chemical building block for bio-based polymers and *C. necator*'s inherent ability to produce such building blocks (e.g., polyhydroxybutyrate, PHB), strain EHCn11, which is unable to fully degrade itaconate, was employed as a chassis for its biosynthesis. Itaconate can be synthesised from the tricarboxylic acid cycle intermediate *cis*-aconitate in a single step, catalysed by *cis*-aconitate decarboxylase (CadA). To achieve itaconate production in *C. necator*, we integrated *Aspergillus terreus cadA* into the *phaCAB* locus, thereby simultaneously disrupting PHB biosynthesis and redirecting carbon flux toward itaconate production (Figure 5A). The correct integration resulting in Δ*phaCAB* P_{araC}-*araC* P_{araBAD}-*cadA* genotype was confirmed by PCR amplification and Sanger sequencing. The resulting strain (EHCn14) was grown under autotrophic conditions in serum bottles, and C5-DCA production was monitored for one week. After one week, an itaconate titre of 9 µM (1.1 mg/L) was obtained. In addition, mesaconate and citramalate were detected at equally low concentrations (1.3 and 3.0 mg/L, respectively). The combined titre of all C5-DCAs reached 278 µM

(Figure 5B), with methylsuccinate as the predominant constituent at 239 µM (31.6 mg/L) (Figure 5C).

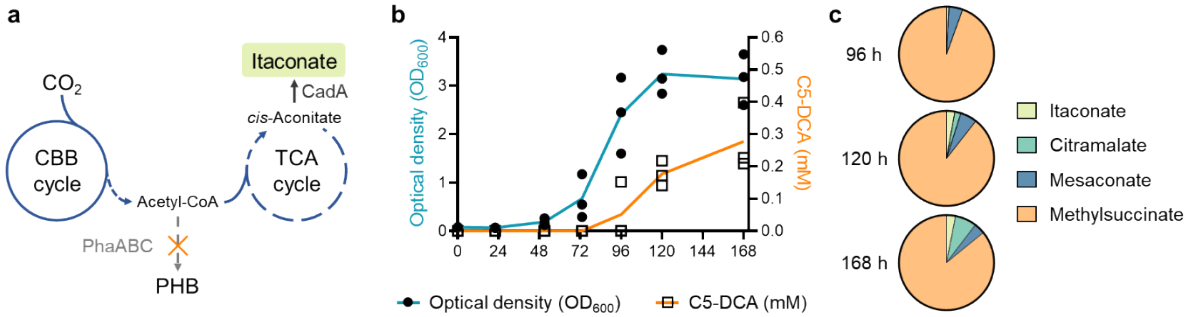

Figure 5. Autotrophic biosynthesis of itaconate in *C. necator*. a Schematic of the CO_2-based itaconate production pathway. The native PHB biosynthesis pathway was replaced with a heterologous *cis*-aconitate decarboxylase CadA. Abbreviations: CBB, Calvin-Benson-Bassham cycle; TCA, tricarboxylic acid cycle. **b** Production of C5-DCAs by strain EHCn14 under autotrophic growth conditions. Data points represent individual biological replicates; lines indicate the average. **c** Average C5-DCA composition at the final three time points, based on titres shown in panel **b**.

Discussion

The microbial production of industrially relevant chemicals from renewable resources is crucial for advancing toward a circular bioeconomy. *C. necator* has emerged as a promising microbial platform for the de novo synthesis of commodity chemicals from CO_2. For instance, its potential has been demonstrated for the autotrophic production of acetoin, 1,3-butanediol, 2,3-butanediol, D-mannitol, and mevalonate[19-22, 42]. While the introduction of a heterologous biosynthetic pathway can redirect metabolic flux toward the target molecule, the biosynthesis of a compound that can be used as a substrate by the host, or is naturally integrated into its metabolic network,

often necessitates substantial genome engineering. In this study, to advance our understanding of itaconate's metabolism and establish the basis for its biosynthesis from CO_2, we mapped an intricate network of enzymes involved in the interconversion and degradation of itaconate and related branched C5-DCAs in *C. necator*.

Based on our analysis of itaconate conversion in various deletion strains, transcriptomic data, homology to established pathways, and acknowledging that intracellular CoA-bound intermediates were not directly measured, we inferred an initial map of itaconate, methylsuccinate, mesaconate, and citramalate metabolism in *C. necator* (Figure 1). Unlike *P. aeruginosa* PAO1, which carries a single operon encoding all essential enzymes for the degradation of itaconate and related C5-DCAs, *C. necator* harbours multiple homologs of the Ict, Ich, Ccl, and Mcd enzymes. All of these homologs were shown to participate in the metabolism of itaconate and related branched C5-DCAs. However, even after deletion of genes encoding the *C. necator* Ict1–4 and Ich1–2 homologs, which exhibit the highest sequence similarity to *P. aeruginosa* Ict and Ich, itaconate was still converted into citramalate, mesaconate, and methylsuccinate. This conversion was reduced when itaconate was supplied extracellularly, but it was nearly complete when itaconate was produced under autotrophic conditions. This observation indicates that *C. necator* may harbour additional enzymes with promiscuous itaconate CoA-transferase and itaconyl-CoA hydratase activities, despite having little or no sequence similarity to PaIct and PaIch.

Some of these enzymes may correspond to candidate genes that were found to be upregulated in response to itaconate supplementation (Figure 4). Additionally, beyond the (*S*)-(*R*)-methylsuccinate isomerase, which allows (*S*)-methylsuccinate to enter the degradation pathway, *C. necator* encodes a protein with high similarity to mesaconate hydratase from *Burkholderia xenovorans*, enabling the interconversion of mesaconate and (*S*)-citramalate (Figure 1)[29]. This putative mesaconate hydratase is encoded by gene *H16_RS12595* (protein sequence identity of 91% and coverage of 98%) and may enable the degradation of mesaconate via (*S*)-citramalate and (3*S*)-citramalyl-CoA.

In addition to the established catabolic pathway proceeding via (*S*)-citramalate and (3*S*)-citramalyl-CoA, our results indicate that residual mesaconate conversion persists even in strains lacking the major Ict and Ich homologs, suggesting the presence of additional, as yet unidentified, enzymatic activities. *C. necator* encodes several proteins with similarity to characterised mesaconate-processing enzymes[43, 44], and although the absence of a functional Ccl homolog likely prevents completion of the canonical (2*R*,3*S*)-β-methylmalyl-CoA pathway (Figure S2)[45], partial flux through a truncated variant of this route cannot be ruled out. Consistent with this, methylsuccinate accumulation following deletion of both methylsuccinyl-CoA dehydrogenases Mcd1 and Mcd2 implies that alternative conversion routes from mesaconate or itaconate to methylsuccinate remain active. At present, two broad mechanistic explanations for the accumulation of

methylsuccinate appear plausible: first, that residual CoA-transferase or hydratase activities enable partial conversion of mesaconate via an incomplete pathway[46]; or second, that itaconate, mesaconate, or their CoA derivatives are directly reduced by an endogenous reductase, as analogous reductions have been reported in other bacteria[47, 48].

Both proposed pathways involve reduction reactions, which decrease the oxidation state of the resulting product methylsuccinate. These reactions require reducing equivalents, such as NAD(P)H, as cofactors. In the wild-type strain, NADPH would typically be consumed for PHB synthesis[19]. In contrast, in the PHB-deficient strain EHCn14, excess NADPH could instead be directed to methylsuccinate production, thereby allowing for NADP+ regeneration. This could explain the pronounced accumulation of methylsuccinate in strain EHCn14 under autotrophic growth conditions.

While we mapped several enzymes involved in the metabolism of itaconate and related C5-DCAs, the transcriptomic analysis revealed 84 genes upregulated by at least fourfold in response to itaconate, methylsuccinate, or mesaconate. Among these, 16 encode proteins with predicted roles in small molecule transport (Table S6).

The branched short-chain dicarboxylate (BSCD) transporter from *P. aeruginosa*, encoded by genes PA0884–PA0886, has been shown to enhance growth on itaconate, mesaconate, (*S*)-citramalate, and both (*S*)- and (*R*)-methylsuccinate when heterologously expressed in *P. putida*[28]. However, no homolog of this transporter could be identified in *C. necator*. Similarly, in

E. coli MG1655, overexpression of the dicarboxylate transporter DctA was found to enhance the conversion of extracellularly supplemented itaconate[27]. Notably, the *C. necator* protein with the highest sequence similarity to DctA (*H16_RS01470*; protein sequence identity of 63% and 98% coverage) was upregulated in response to itaconate and mesaconate supplementation, suggesting a potential role in their uptake.

Furthermore, while we confirmed the involvement of ItcR1 in controlling gene expression primarily in response to itaconate, elevated expression of *operon1* and *mcd2* was observed in the presence of methylsuccinate. Moreover, *operon3* was activated in response to mesaconate, indicating a more intricate transcriptional regulatory network. For example, the LysR-type transcriptional regulator encoded by gene *H16_RS25575* is the closest homolog to PaItcR (50% protein sequence identity, 98% coverage). Although its genomic proximity to *mcd2* suggests a role in its transcriptional regulation, its natural ligand and target promoters remain to be experimentally validated.

This expanded regulatory landscape, coupled with residual catabolic capacity, has direct implications for redirecting carbon flux toward itaconate. While the itaconate titre obtained here under autotrophic conditions is low compared to highly efficient heterotrophic bioprocesses in fungi such as *Aspergillus terreus*, the functional and regulatory insights presented in this study outline clear and actionable routes for redirecting carbon flux toward itaconate in future work. Our transcriptomic analysis revealed several

candidate genes encoding enzymes with potential roles in C5-DCA interconversion, transcriptional regulators that may govern C5-DCA metabolism, and putative transporter proteins. Targeted perturbation of these nodes, by deletion or downregulation, could alter the distribution of C5-DCAs, facilitate export of desired products, or limit re-uptake, thereby improving selectivity for itaconate. Additional opportunities arise from adjusting intracellular redox balance, particularly under autotrophic conditions, to enable cofactor regeneration without diverting carbon toward the reductive branches of the pathway that drive methylsuccinate accumulation.

Conclusions

This study represents a first step toward unravelling the metabolic pathways of itaconate and related branched C5-DCAs in *C. necator* H16 and establishing it as a microbial platform for their biosynthesis from CO_2. Moreover, our findings highlight *C. necator* as a rich source of proteins with catalytic, regulatory, and transport functions involved in itaconate, methylsuccinate, mesaconate, and citramalate metabolism, providing valuable tools for metabolic engineering aimed at optimising their biosynthesis.

Declarations

Ethics approval and consent to participate

Not applicable.

Consent for publication

Not applicable.

Availability of data and materials

RNAseq data have been deposited at GEO (https://www.ncbi.nlm.nih.gov/geo/) under accession number GSE314393 and are publicly available as of the date of publication. All unique/stable reagents generated in this study will be made available on request, but we may require a payment and/or a completed materials transfer agreement if there is potential for commercial application.

Competing interests

The authors have no conflicts of interest to declare.

Funding

This project has received funding from Research Council of Lithuania (LMTLT), agreement no. S-MIP-24-48 (to NM).

Author contributions

EKRH: conceptualisation, formal analysis, investigation, methodology, validation, visualisation, writing – original draft; NM: conceptualisation, funding acquisition, investigation, methodology, project administration, supervision, validation, writing – review and editing.

Acknowledgements

This project has received funding from Research Council of Lithuania (LMTLT), agreement no. S-MIP-24-48 (to NM). EKRH acknowledges support from the Biotechnology and Biological Sciences Research Council (BBSRC;

grant number BB/L013940/1), and the Engineering and Physical Sciences Research Council (EPSRC) under the same grant number, and the Future Biomanufacturing Research Hub (grant EP/S01778X/1), funded by the EPSRC and BBSRC as part of UK Research and Innovation (UKRI).

References

1. Michelucci, A., et al., *Immune-responsive gene 1 protein links metabolism to immunity by catalyzing itaconic acid production.* Proceedings of the National Academy of Sciences, 2013. **110**(19): p. 7820-7825.
2. McGettrick, A., et al., *Metabolic messengers: itaconate.* Nature metabolism, 2024. **6**(9): p. 1661-1667.
3. Werpy, T. and G. Petersen, *Top Value Added Chemicals from Biomass: Volume I -- Results of Screening for Potential Candidates from Sugars and Synthesis Gas*. 2004, National Renewable Energy Lab. (NREL), Golden, CO (United States): United States.
4. Robert, T. and S. Friebel, *Itaconic acid–a versatile building block for renewable polyesters with enhanced functionality.* Green Chemistry, 2016. **18**(10): p. 2922-2934.
5. Teleky, B.-E. and D.C. Vodnar, *Biomass-derived production of itaconic acid as a building block in specialty polymers.* Polymers, 2019. **11**(6): p. 1035.
6. Zhang, J., et al., *Itaconic acid-based hyperbranched polymer toughened epoxy resins with rapid stress relaxation, superb solvent resistance and closed-loop recyclability.* Green Chemistry, 2022. **24**(18): p. 6900-6911.
7. Kolář, M., et al., *Utilization of Bio-based Monomer Derived from Camelina Oil and Itaconic Acid for the Synthesis of Film-forming Latexes.* Journal of Polymers and the Environment, 2025: p. 1-18.
8. Bonnarme, P., et al., *Itaconate biosynthesis in Aspergillus terreus.* Journal of bacteriology, 1995. **177**(12): p. 3573-3578.
9. Wierckx, N., et al., *Metabolic specialization in itaconic acid production: a tale of two fungi.* Current opinion in biotechnology, 2020. **62**: p. 153-159.
10. Hevekerl, A., A. Kuenz, and K.-D. Vorlop, *Influence of the pH on the itaconic acid production with Aspergillus terreus.* Applied microbiology and biotechnology, 2014. **98**(24): p. 10005-10012.
11. Blazeck, J., et al., *Metabolic engineering of Yarrowia lipolytica for itaconic acid production.* Metabolic engineering, 2015. **32**: p. 66-73.
12. Harder, B.-J., K. Bettenbrock, and S. Klamt, *Model-based metabolic engineering enables high yield itaconic acid production by Escherichia coli.* Metabolic engineering, 2016. **38**: p. 29-37.
13. Geiser, E., et al., *Ustilago maydis produces itaconic acid via the unusual intermediate trans-aconitate.* Microbial biotechnology, 2016. **9**(1): p. 116-126.
14. Young, E.M., et al., *Iterative algorithm-guided design of massive strain libraries, applied to itaconic acid production in yeast.* Metabolic Engineering, 2018. **48**: p. 33-43.

15. Elkasaby, T., et al., *Co-utilization of maltose and sodium acetate via engineered Corynebacterium glutamicum for improved itaconic acid production.* Biotechnology and Bioprocess Engineering, 2023. **28**(5): p. 790-803.
16. Severinsen, M.M., et al., *Efficient production of itaconic acid from the single-carbon substrate methanol with engineered Komagataella phaffii.* Biotechnology for Biofuels and Bioproducts, 2024. **17**(1): p. 98.
17. Claassens, N.J., et al., *Harnessing the power of microbial autotrophy.* Nature Reviews Microbiology, 2016. **14**(11): p. 692-706.
18. Weldon, M. and C. Euler, *Physiology-informed use of Cupriavidus necator in biomanufacturing: a review of advances and challenges.* Microbial Cell Factories, 2025. **24**(1): p. 30.
19. Gascoyne, J.L., et al., *Engineering Cupriavidus necator H16 for the autotrophic production of (R)-1, 3-butanediol.* Metabolic engineering, 2021. **67**: p. 262-276.
20. Bommareddy, R.R., et al., *A sustainable chemicals manufacturing paradigm using CO_2 and renewable H_2.* Iscience, 2020. **23**(6).
21. Hanko, E.K., et al., *Biosensor-informed engineering of Cupriavidus necator H16 for autotrophic D-mannitol production.* Metabolic Engineering, 2022. **72**: p. 24-34.
22. Garavaglia, M., et al., *Stable platform for mevalonate bioproduction from CO_2.* ACS Sustainable Chemistry & Engineering, 2024. **12**(36): p. 13486-13499.
23. Wang, S.-F., J. Adler, and H.A. Lardy, *The pathway of itaconate metabolism by liver mitochondria.* Journal of Biological Chemistry, 1961. **236**(1): p. 26-30.
24. Cooper, R. and H. Kornberg, *The utilization of itaconate by Pseudomonas sp.* Biochemical Journal, 1964. **91**(1): p. 82.
25. Sasikaran, J., et al., *Bacterial itaconate degradation promotes pathogenicity.* Nature chemical biology, 2014. **10**(5): p. 371-377.
26. Hanko, E.K., N.P. Minton, and N. Malys, *A transcription factor-based biosensor for detection of itaconic acid.* ACS Synthetic Biology, 2018. **7**(5): p. 1436-1446.
27. Lee, S.H., P.C. Cirino, and R. Gonzalez, *Metabolic engineering of Escherichia coli for the utilization of methylsuccinate, the product of methane activation via fumarate addition.* Bioresource Technology, 2025. **416**: p. 131700.
28. de Witt, J., et al., *Characterization and engineering of branched short-chain dicarboxylate metabolism in Pseudomonas reveals resistance to fungal 2-hydroxyparaconate.* Metabolic Engineering, 2023. **75**: p. 205-216.
29. Kronen, M., J. Sasikaran, and I.A. Berg, *Mesaconase activity of class I fumarase contributes to mesaconate utilization by Burkholderia xenovorans.* Applied and environmental microbiology, 2015. **81**(16): p. 5632-5638.
30. Gonner, L., et al., *Pseudomonadal itaconate degradation gene cluster encodes enzymes for methylsuccinate utilization.* Communications Biology, 2025. **8**(1): p. 1099.
31. Simon, R., U. Priefer, and A. Pühler, *A broad host range mobilization system for in vivo genetic engineering: transposon mutagenesis in gram negative bacteria.* Nature Biotechnology, 1983. **1**(9): p. 784-791.
32. Sambrook, J. and D.W. Russell, *Molecular cloning: a laboratory manual*. Vol. 1. 2001: Cold Spring Harbor Laboratory Cold Spring Harbor, NY.
33. Lenz, O., et al., *The Alcaligenes eutrophus H16 hoxX gene participates in hydrogenase regulation.* Journal of Bacteriology, 1994. **176**(14): p. 4385-4393.

34. Schlegel, H., H. Kaltwasser, and G. Gottschalk, *Ein Submersverfahren zur Kultur wasserstoffoxydierender Bakterien: Wachstumsphysiologische Untersuchungen.* Archiv für Mikrobiologie, 1961. **38**(3): p. 209-222.
35. Trüper, H.G. and N. Pfennig, *Characterization and identification of the anoxygenic phototrophic bacteria*, in *The Prokaryotes*. 1981, Springer. p. 299-312.
36. Ausubel, F.M., et al., *Current Protocols in Molecular Biology*. 2003: John Wiley & Sons.
37. Hanko, E.K., N.P. Minton, and N. Malys, *Characterisation of a 3-hydroxypropionic acid-inducible system from Pseudomonas putida for orthogonal gene expression control in Escherichia coli and Cupriavidus necator.* Scientific reports, 2017. **7**(1): p. 1724.
38. Schwartz, E., et al., *A proteomic view of the facultatively chemolithoautotrophic lifestyle of Ralstonia eutropha H16.* Proteomics, 2009. **9**(22): p. 5132-5142.
39. Altschul, S.F., et al., *Gapped BLAST and PSI-BLAST: a new generation of protein database search programs.* Nucleic acids research, 1997. **25**(17): p. 3389-3402.
40. Riquelme, S.A., et al., *Pseudomonas aeruginosa utilizes host-derived itaconate to redirect its metabolism to promote biofilm formation.* Cell metabolism, 2020. **31**(6): p. 1091-1106.
41. Schürmann, M., et al., *Novel reaction of succinyl coenzyme A (succinyl-CoA) synthetase: activation of 3-sulfinopropionate to 3-sulfinopropionyl-CoA in Advenella mimigardefordensis strain DPN7T during degradation of 3, 3′-dithiodipropionic acid.* Journal of bacteriology, 2011. **193**(12): p. 3078-3089.
42. Windhorst, C. and J. Gescher, *Efficient biochemical production of acetoin from carbon dioxide using Cupriavidus necator H16.* Biotechnology for biofuels, 2019. **12**: p. 1-11.
43. Borjian, F., et al., *Succinyl-CoA: mesaconate CoA-transferase and mesaconyl-CoA hydratase, enzymes of the methylaspartate cycle in Haloarcula hispanica.* Frontiers in Microbiology, 2017. **8**: p. 1683.
44. Zarzycki, J., et al., *Mesaconyl-coenzyme A hydratase, a new enzyme of two central carbon metabolic pathways in bacteria.* Journal of bacteriology, 2008. **190**(4): p. 1366-1374.
45. Herter, S., A. Busch, and G. Fuchs, *L-Malyl-coenzyme A lyase/β-methylmalyl-coenzyme A lyase from Chloroflexus aurantiacus, a bifunctional enzyme involved in autotrophic CO2 fixation.* Journal of bacteriology, 2002. **184**(21): p. 5999-6006.
46. Wang, J., et al., *Microbial production of branched-chain dicarboxylate 2-methylsuccinic acid via enoate reductase-mediated bioreduction.* Metabolic engineering, 2018. **45**: p. 1-10.
47. Li, J., et al., *Asymmetric synthesis of both enantiomers of dimethyl 2-methylsuccinate by the ene-reductase-catalyzed reduction at high substrate concentration.* Catalysts, 2022. **12**(10): p. 1133.
48. Little, A.S., et al., *Dietary-and host-derived metabolites are used by diverse gut bacteria for anaerobic respiration.* Nature microbiology, 2024. **9**(1): p. 55-69.